1661-8726/07/010053-18
DOI 10.1007/s00015-007-1211-7
Birkhäuser Verlag, Basel, 2007

Swiss j. geosci. 100 (2007) 53–70

Structural geology and petrography of the Naret region (northern Valle Maggia, N. Ticino, Switzerland)

ANDREA GALLI[1], NEIL MANCKTELOW[2], ERIC REUSSER[1] & MARK CADDICK[1]

Key words: Maggia nappe, Lebendun nappe, Matorello gneiss, tectono-metamorphic evolution of the Central Alps

ABSTRACT

The Naret region has a complex geological history of Alpine polyphase folding and metamorphism that affected pre-Alpine rocks of the Maggia nappe, including the Matorello group (interpreted in this study as late-Variscan intrusives), the Lebendun nappe and Mesozoic rocks of the Bedretto zone. From field observations, four main ductile deformation phases (D_1 to D_4) can be distinguished and, in combination with thermodynamic modelling, the tectono-metamorphic evolution for the Naret region can be reconstructed. D_1 formed the initial nappe stack. During this phase, the Maggia nappe was thrust over the Lebendun nappe, at T ≤ 570°C and P ≤ 10 kbar. D_2 caused isoclinal refolding of the nappe pile, at around 610–640°C and 8.5–10 kbar, and produced both the main regional foliation (S_2) and a penetrative stretching lineation which is generally parallel to F_2 fold axes. D_2 is largely responsible for the current complicated geometry of the Lebendun nappe boundary. The main phase of porphyroblastesis occurred between D_2 and D_3, corresponding to a metamorphic temperature peak of ca. 640–650°C at pressures of ca. 8–9 kbar. D_3 produced open folds oblique to the general Alpine trend ("crossfolding") and locally a crenulation cleavage with a well developed crenulation lineation, at estimated temperatures of 550–610°C. The last important phase, D_4, caused open backfolding of all pre-existing structures and is responsible for steepening of the main S_2 foliation, to produce the Northern Steep Zone, and for a regional rotation of S_3 and L_3. D_4 developed at T ≥ 550°C and P ≥ 3 kbar.

The Lebendun nappe is a complicated structure developed as the result of non-coaxial fold interference related to D_1 and D_2. From tectono-stratigraphic evidence, the rocks of the Lebendun nappe are interpreted as pre-Triassic in age.

1. Introduction

The area around Lago del Naret, located in the northern Lepontine Alps (Fig. 1), is a classic region for studies of polyphase folding and its relationship to mineral growth (Ramsay 1967; Ayrton & Ramsay 1974; Klaper 1982; Ramsay & Huber 1987; Grujic 1993) and of heterogeneous simple shear development (Ramsay & Graham 1970; Ramsay & Allison 1979; Simpson 1981, 1982a; Mohanty & Ramsay 1994). In terms of Alpine geology, it is also a critical region for establishing the tectonic history of the Central Alps, because the well-developed fold interference patterns allow the sequence of geometrically distinct deformation events to be distinguished unequivocally (e.g. Grujic & Mancktelow 1996). However, this zone presents several geological problems that are still unresolved. The major controversies concern the structural evolution and tectono-stratigraphic position of the Lebendun and Maggia nappes (Niggli et al. 1936; Steck & Hunziker 1994; Grujic & Mancktelow 1996; Froitzheim et al. 1996; Steck 1998; Schmid et al. 2004; Maxelon & Mancktelow 2005), the Permo-Carboniferous versus Mesozoic age of conglomeratic rocks assigned to the Lebendun nappe (Rodgers & Bearth 1960; Spring et al. 1992), and the magmatic source of the Matorello orthogneiss (Günthert et al. 1976, 1996; Ramsay & Allison 1979). In the current study, the Naret region was remapped on a scale of 1:10'000, with particular emphasis on structural relationships and the interplay between deformation and metamorphism. Field and thin-section observations establish that the structural history may be described in terms of four geometrically and kinematically distinct deformation phases. In combination with thermodynamic modelling, a tectono-meta-

[1] Institute for Mineralogy and Petrography, ETH Zürich, 8092 Zürich, Switzerland
[2] Institute for Geology, ETH Zürich, 8092 Zürich, Switzerland
Corresponding author: E. Reusser. E-mail: reusser@erdw.ethz.ch

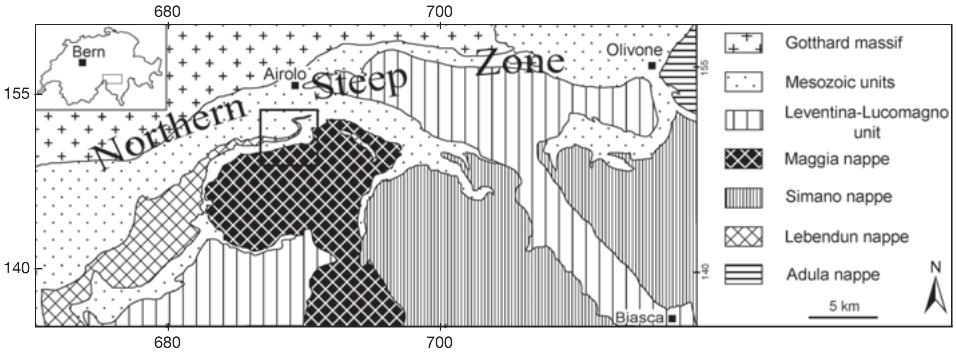

Fig. 1. Tectonic map of the northern Lepontine Alps, showing the main tectonic units and the position of the Northern Steep Zone (Milnes, 1974b). Swiss co-ordinates are given with units in kilometres. Inset outlines the study area.

morphic history could be determined that is common to all units in the Naret region. The structural position of the Lebendun nappe is discussed, based on a geometric model of its relatively complex shape that is consistent with observed small-scale parasitic fold vergences and fold overprinting relationships. Conglomerates associated with the Lebendun nappe do not outcrop in the area mapped for this study. However, the position of the more even-grained meta-arkosic paragneisses forming the "crystalline core" of the Lebendun gneiss in the Naret region is discussed and arguments supporting a pre-Mesozoic age are presented. The magmatic history of the Matorello gneiss within the Maggia nappe is considered in detail and field evidences are presented to support a plutonic intrusive origin for this body rather than local melting of adjacent paragneisses.

2. Geological setting

The Naret region is part of the Lower Pennine Zone (Milnes 1974b). It is located in the Northern Steep Zone (Milnes 1974b) where all tectonic units – including the Gotthard massif, its para-autochthonous sedimentary cover and the Lower Pennine Zone – are in a subvertical position. The Naret region comprises three tectonic units (Fig. 1): the northern and frontal part of the Maggia nappe, the eastern part of the Lebendun nappe and the Bedretto zone, which consists of metasediments representing the original Mesozoic cover of both nappes. In the Central Alps, Mesozoic metasedimentary units form mappable marker horizons separating the different crystalline nappes (Schmid & Preiswerk 1908; Preiswerk 1918).

The Maggia nappe is composed of pre-Mesozoic orthogneisses, paragneisses and schists. It also includes the Matorello body, which is a late-Variscan, 300 Ma old intrusion (Köppel et al. 1981a) located in the core of the nappe. The orthogneisses represent pre-Variscan intrusions, as established from dating of similar orthogneisses at Alpe Scheggia, 6–7 km to the east (Steiner 1984a), which yielded a magmatic Rb/Sr age of 430-580 Ma. Studies of the metasedimentary rocks by Köppel et al. (1981a,b) identified two zircon populations, the first of pre-Caledonian age and the second with an age between Caledonian and Variscan time. The tectono-stratigraphic position of the Maggia nappe is still controversial. Froitzheim et al. (1996) and Schmid et al. (2004) assigned the Maggia nappe to the Briançonnais (or Middle Penninic) domain. In contrast, Maxelon & Mancktelow (2005) argued that the Maggia and Simano nappes are part of the same unit, supporting an assignment to the thinned passive margin of the European continent.

The Lebendun nappe is a sequence of orthogneisses and conglomeratic to psammitic metasediments (Schmid & Preiswerk 1908; Bearth 1973; Spring et al. 1992). The age of the metasediments is still controversial. Rodgers and Bearth (1960) suggested that the Lebendun conglomerates and sandstones represent a series of flysch-like sediments deposited in Mesozoic time. This interpretation was supported by Spring et al. (1992), who proposed three possible paleogeographic environments ranging from Lias-Dogger to Cretaceous-Tertiary in age. In contrast, Wenk & Günthert (1960), Milnes (1964, 1965), Joos (1969), Bearth (1973) and Leu (1986) suggested a pre-Triassic (possibly Permo-Carboniferous) age, mainly based on their field observations suggesting that the Lebendun conglomeratic metasediments are typically overlain by quartzites and dolomitic marbles of probable Triassic age.

The Bedretto zone consists of calcitic and dolomitic marbles of Triassic age, as well as a very heterogeneous series of calc-micaschists of probable Jurassic age (Steinmann 1994), often referred to as "Bündnerschiefer".

All of these units were involved in intense polyphase deformation and metamorphism during the Alpine orogeny (Ayrton & Ramsay 1974; Milnes 1974a,b; Klaper 1980, 1982; Huber et al. 1980; Huber 1981; Simpson 1982b; Grujic 1992; Grujic & Mancktelow 1996; Maxelon & Mancktelow 2005). Alpine metamorphism in the Naret region reached peak conditions of lower to middle amphibolite facies (Niggli & Niggli 1965), characterised by the presence of kyanite and staurolite in metapelitic series and by the presence of tremolite + calcite in impure dolomitic marbles (Trommsdorff 1966). Overall there is a steady increase in metamorphic grade from north to south in the Central Alps (e.g. Niggli & Niggli 1965), but the metamorphic gradient is not constant. From the Aar and Gotthard massifs in the north into the adjacent para-autocthonous sedimentary cover to the south, there is a strong gradient in metamorphic grade from greenschist to lower amphibolite facies

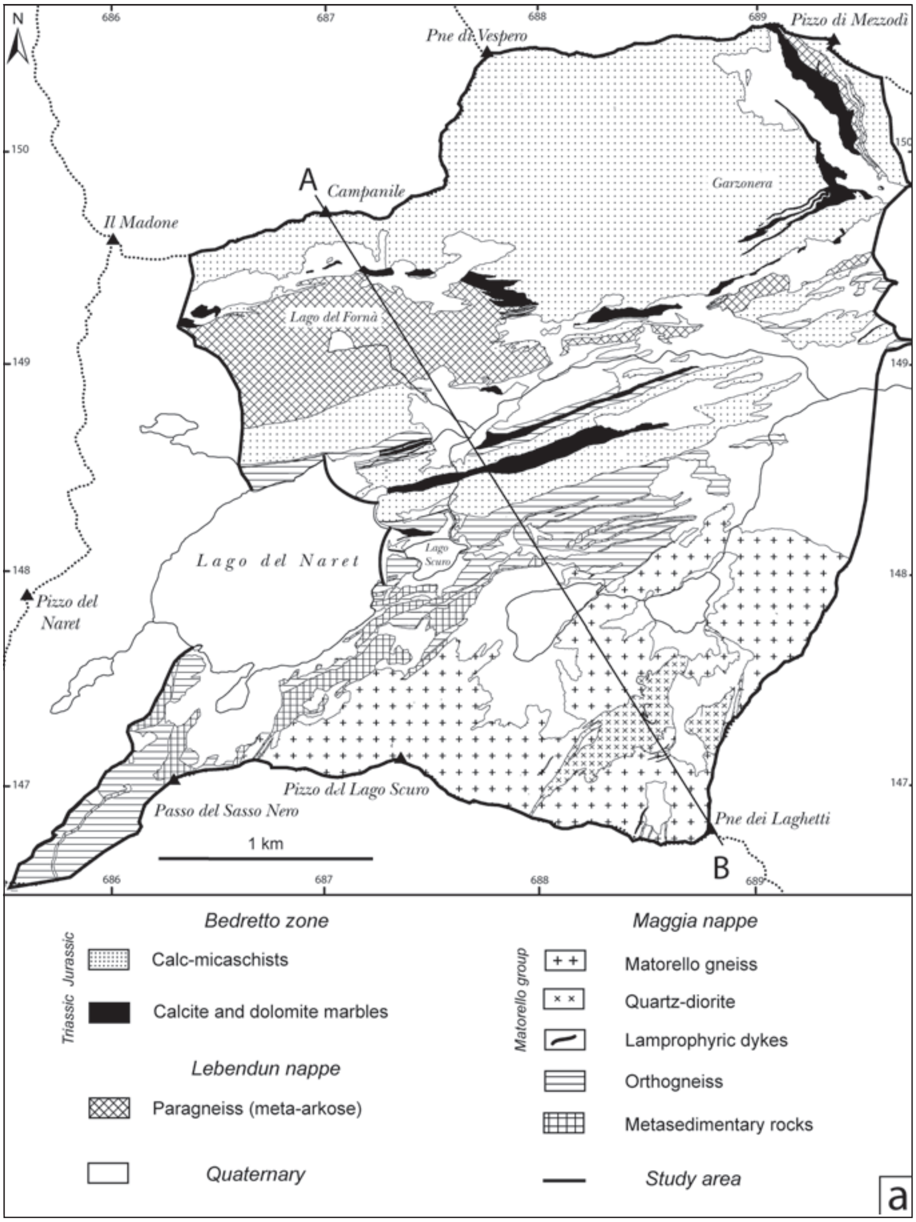

Fig. 2. a) Geological map of the Naret region, with the boundary of the mapped area indicated by a thick black line. A–B: location of the profile in Fig. 3.

(Klaper 1982, 1985) whereas further south in the northern Pennine zone, where the studied area is located, the north-south gradient in the metamorphic conditions is weak (Niggli & Niggli 1965; Gunzenreiner 1998; Albisetti 1999; Allaz & Mader, 2003 and Rütti 2003).

3. Petrographical characterisation of the mapped units

During this study, a 10 km^2 area has been mapped on the scale 1:10'000. Rocks of the Maggia nappe occur in the south of the map area, rocks of the Lebendun nappe in the central part, and Mesozoic rocks of the Bedretto zone mark the separation between these two nappes as well as dominating the northern part of the map area (Figs. 2a, 3).

3.1. Maggia nappe

The *orthogneisses* (Fig. 4a) are characterised by porphyroclasts of K-feldspar and quartz ("augengneiss"). Their modal composition is relatively homogeneous and they typically contain quartz-plagioclase-K-feldspar-muscovite-biotite, with epidote, chlorite, apatite, rutile, ilmenite and idiomorphic zircon as accessories. Two types of orthogneiss can be distinguished, one with porphyroclasts of up to 1 cm size, the other with very coarse, up to 4 cm sized porphyroclasts. Both types have sharp boundaries to the other rock types.

The *metasedimentary rocks* include strongly foliated and compositionally heterogeneous pelitic micaschists and psammitic paragneisses (Fig. 4b), with gradational boundaries

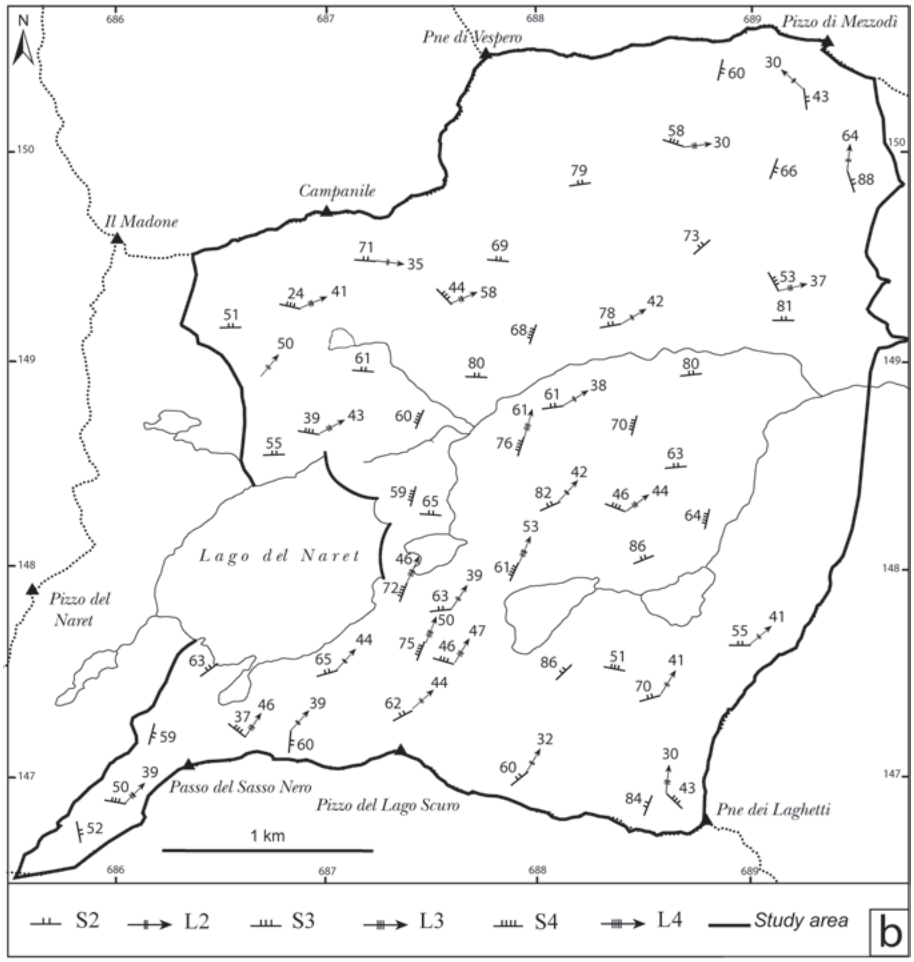

Fig. 2. b) Structural map of the Naret region showing the orientation of representative S_2 (main foliation), S_3 (D_3 fold axial plane), S_4 (D_4 fold axial plane), L_2 (mineral/stretching lineation), L_3 (crenulation lineation), L_4 (D_4 fold axis). Swiss co-ordinates are given in units of kilometres.

between lithologies. Mineral assemblages typically contain quartz-plagioclase-biotite-muscovite-garnet ± staurolite and tourmaline. Epidote, chlorite, titanite, rutile, apatite, graphite, zircon and ilmenite occur as accessories.

The *Matorello body* is subdivided into the Matorello gneiss, a quartz-diorite, and lamprophyric, aplitic and pegmatitic dykes. The *Matorello gneiss* (Fig. 4c) is a grey leucocratic granite forming the main body of the intrusion. The homogeneous modal composition has produced quartz-plagioclase-K-feldspar-biotite, with epidote, muscovite, chlorite, titanite, apatite, zircon and allanite as accessories. Mafic rocks occur as both isolated enclaves and as enclave swarms. The *quartz-diorite* (Fig. 4d) is a dark green, coarse-grained and massive basic rock body of ca. 1 km length and ca. 400 m width, occurring within the Matorello gneiss (Figs. 2a, 3). The mineral assemblage consists of dark green amphibole (tschermakitic hornblende)-biotite-plagioclase-quartz-epidote ± titanite, chlorite, apatite and rutile. Despite the regionally strong Alpine deformation, the quartz-diorite remains practically undeformed and preserves the original gabbroic texture. The *lamprophyric dykes*, which were studied previously by Steiner (1984b), are 5–15 m thick, dark green, coarse-grained intrusions. They occur in both the Matorello gneiss and the quartz-diorite, and contain green amphibole (actinolitic hornblende)-epidote-chlorite-plagioclase-quartz-phlogopite ± titanite and apatite. The *aplitic dykes* are 50–100 cm thick, fine-grained, weakly foliated, leucocratic granites. In general, they are composed of quartz-plagioclase-K-feldspar-biotite. Locally, aplites exhibit elongated aggregates of coarse tourmaline, outlining the main stretching lineation L_2 (Fig. 5a). These aggregates are 5–6 cm long and 1–2 cm wide, and are surrounded by ca. 0.5 cm haloes of biotite-free aplite (Fig. 5b). The *pegmatitic dykes* are 0.5–1.5 m thick and are composed of quartz-plagioclase-K-feldspar-muscovite-tourmaline. Idiomorphic tourmaline crystals within the pegmatites can reach 15 cm in size.

3.2. Lebendun nappe

The Lebendun nappe consists of a suite of foliated metasediments of arkosic origin (Fig. 4e), all of which have a similar mineral assemblage containing quartz-plagioclase-K-feldspar-biotite-muscovite-calcite, with epidote, garnet, apatite, chlo-

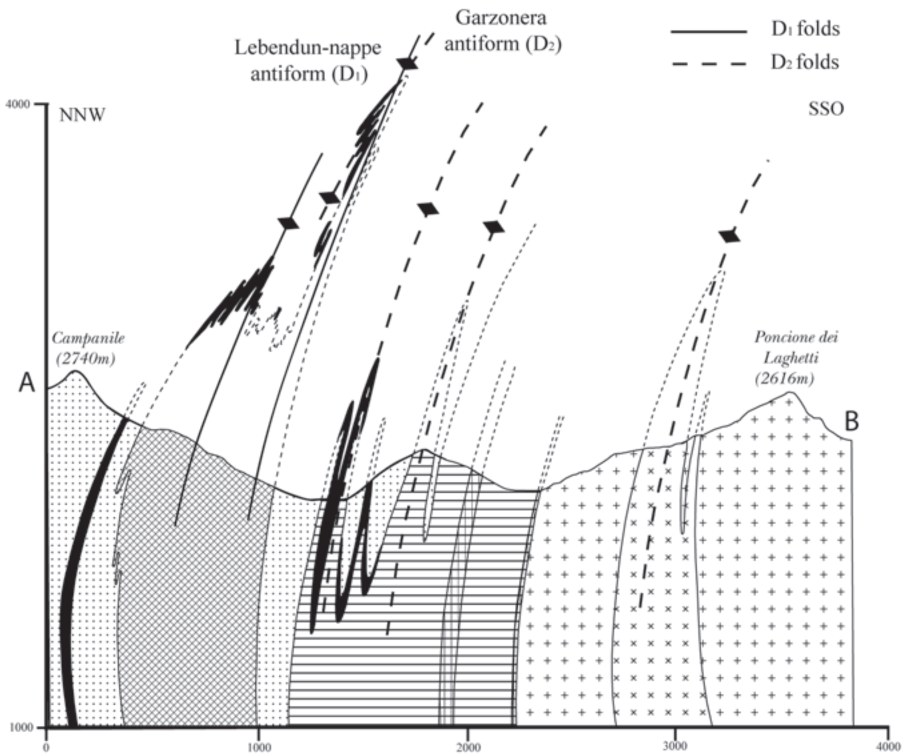

Fig. 3. Geological profile through the studied area, drawn from Campanile to Poncione dei Laghetti (trace A–B on Fig. 2). Units are metres. Lithological signatures are the same as in Fig. 2.

rite, zircon and ilmenite as accessories. Modal compositions vary and grain sizes range from ≤ 0.5mm up to ca 7mm. In contrast to adjacent regions further west (Burckhardt 1942; Günthert 1954a,b; Rodgers & Bearth 1960; Wenk & Günthert 1960; Milnes 1964, 1965; Joos 1969; Bearth 1973; Huber-Aleffi 1982), there are no obvious meta-conglomerates within the Lebendun nappe in the mapped area.

3.3. Bedretto zone

3.3.1. Metacarbonates (Triassic)

The metacarbonates occur as thin (<100 m wide) bands between the two crystalline nappes (Fig. 3) and, based on regional lithological correlations, are most probably of Triassic age. The predominant lithology is calcite marble, containing calcite-quartz-plagioclase-muscovite. Tremolite-bearing dolomite marbles and rauhwackes are also observed, but are less common.

3.3.2. Calc-micaschists

The calc-micaschists (Fig. 4f) are a heterogeneous series of alternating pelites, psammites and carbonate material. Band thicknesses are variable and all rocks are strongly foliated. Typical mineral assemblages contain quartz-plagioclase-calcite-biotite-muscovite-garnet-epidote-graphite ± chlorite, tourmaline, titanite, rutile and ilmenite, although intercalations of calcite-free metapelites also occur locally and contain cm-sized porphyroblasts of garnet, staurolite and kyanite (Figs. 6a, 6b). Meta-sandstone lenses composed of quartz-plagioclase-muscovite also occur, but are relatively uncommon.

4. The Matorello intrusion

4.1. Magma genesis

The origin of the magma of the Matorello intrusion is controversial. Günthert et al. (1976, 1996) suggested local anatexis of paragneisses during the Variscan orogenesis, triggered by syntectonic Variscan ultrametamorphism. However, we consider the Matorello rocks to represent a late-Variscan primary intrusion, in agreement with Ramsay & Allison (1979). Several field observations support this interpretation: (i) the sharp intrusive boundaries between the Matorello gneiss and the country rocks, (ii) the occurrence of mafic enclaves of quartz-dioritic composition in the Matorello gneiss, (iii) the appearance of mafic dykes transforming into swarms of mafic enclaves as a result of magma mingling (Fig. 7), (iv) the occurrence of stoping features (Fig. 8), and (v) the occurrence of late intrusive aplitic and pegmatitic dykes.

The mineralogy of the Matorello gneiss (biotite granite) suggests its origin as a differentiated mantle magma, i.e. an I-type granite, since S-type granites may be expected to develop biotite + muscovite ± garnet (Chapell & White 1974).

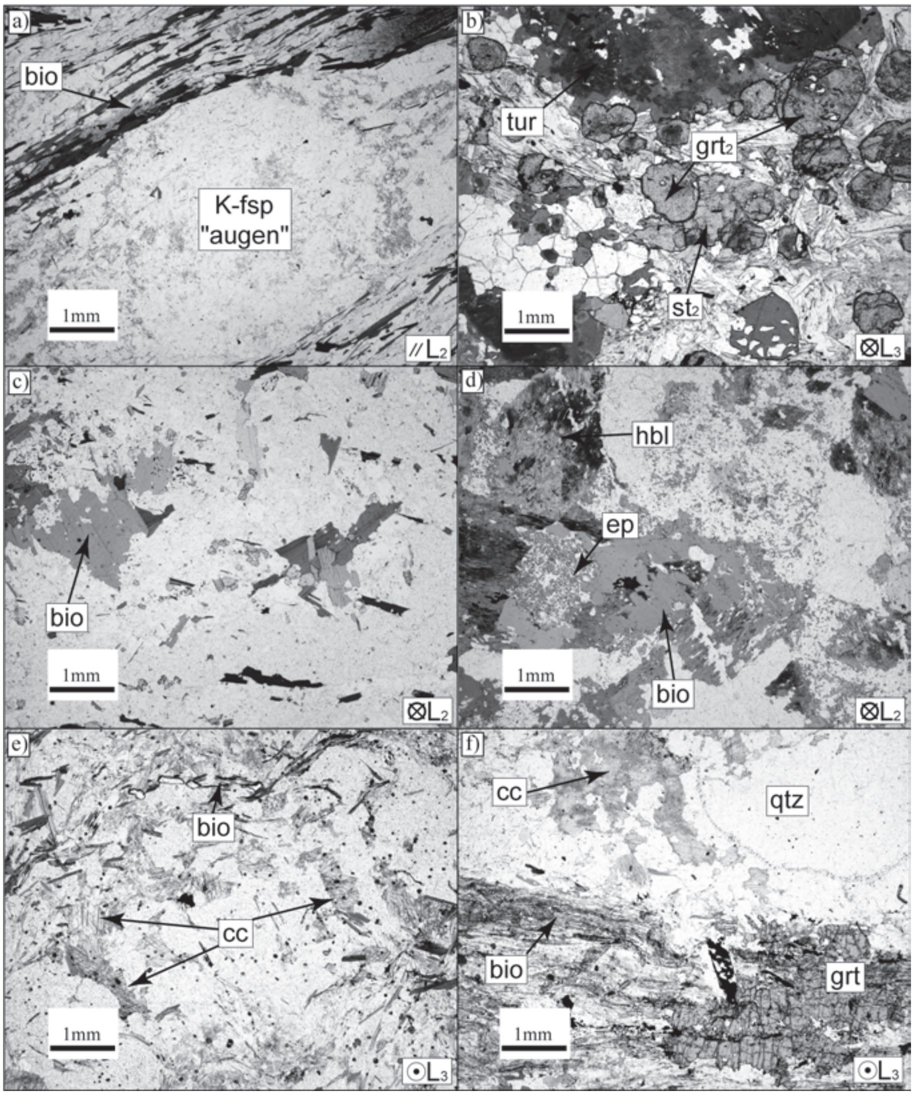

Fig. 4. Photomicrographs of the studied rock types. a) Orthogneiss of the Maggia nappe, with coarse grained K-feldspar-"augen". b) Metapelitic tourmaline-staurolite-garnet-biotite-schist (Maggia nappe), showing mineral equilibrium between garnet-staurolite-tourmaline. c) Matorello gneiss (Maggia nappe), showing large unoriented biotites. d) Porphyric hornblende, epidote and biotite in quartz-diorite (Maggia nappe). e) Calcite-bearing meta-arkose of the Lebendun nappe. f) Garnet-bearing calc-micaschists of the Bedretto Zone. All photomicrographs with plane polarised light. The symbols in the lower right corners define the orientation of the lineation with respect to the thin section. // = L parallel to the thin section plane; ⊗ = L perpendicular to the thin section plane, view direction down-dipping; ⊙ = L perpendicular to the thin section plane, view direction up-pointing.

4.2. Mechanism and sequence of intrusion

From crosscutting relationships, the first intrusion was the quartz-diorite, which was followed by granite (i.e. the Matorello gneiss), and then the lamprophyric, aplitic, and finally, pegmatitic dykes. The field characteristics of the quartz-diorite and its relationship to the Matorello gneiss suggest that overhead stoping is the most likely intrusion mechanism for the granitic rock. The granitic magma has infiltrated the pre-existing quartz-diorite along fractures, forming an in-situ breccia and allowing melt to migrate. With progressive fracturing of the quartz-diorite, an interconnected network of granitic magma developed around more isolated blocks of quartz-diorite, leading to the development of rounded mafic enclaves (Figs. 8a–d).

A second type of mafic enclave within the Matorello gneiss occurs as swarms (Fig. 7) that progressively develop from more coherent lamprophyric dykes and are interpreted to have developed due to mingling of two magmas, as the lamprophyric dyke intruded into still (partially) molten granitic magma (cf. Hill 1984).

5. Structural geology

Four main Alpine deformation phases can be distinguished in the Naret region, based on overprinting relationships.

5.1. Deformation phase D_1

D_1 is related to the initial nappe stacking phase and forms large isoclinal folds with crystalline cores surrounded by Mesozoic rocks (e.g. Ayrton & Ramsay 1974). Overprint by subsequent deformation phases makes the determination of the original D_1-fold geometry difficult. Only in the Matorello

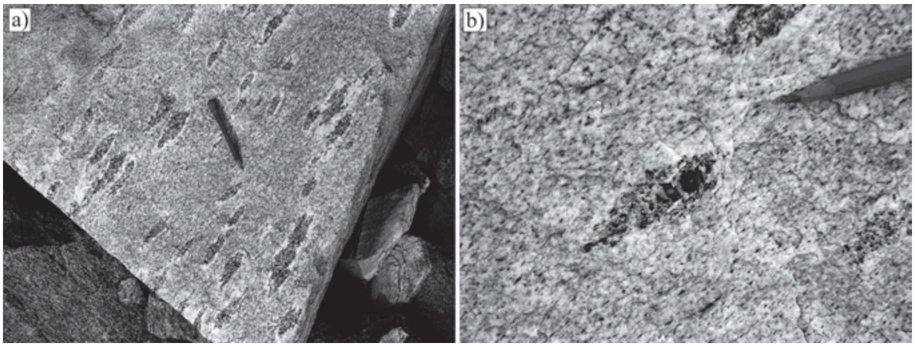

Fig. 5. a) Boulder of a deformed aplitic dyke with elongated tourmaline aggregates (Pne dei Laghetti, Swiss co-ordinates 688'815/147'090). b) Detail of a stretched tourmaline aggregate, defining L_2.

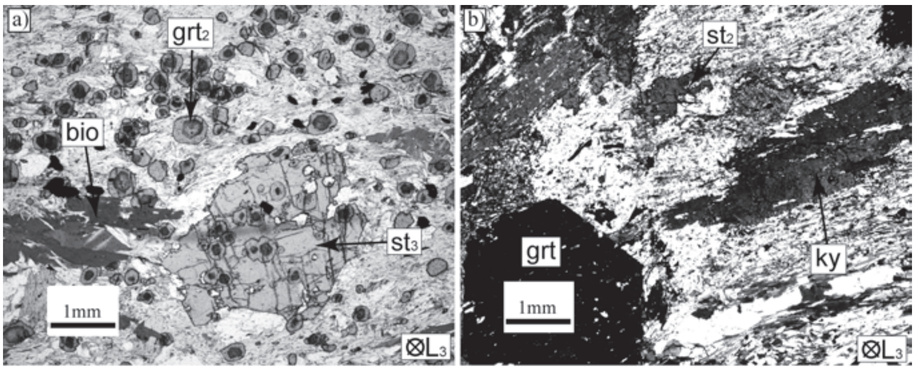

Fig. 6. Photomicrographs of the metapelitic bands in calc-micaschists of the Bedretto zone. a) Staurolite and garnet porphyroblasts in staurolite-garnet-schist (plane polarised light). b) Garnet, staurolite and kyanite porphyroblasts in kyanite-staurolite-garnet-schist (crossed polarised light).

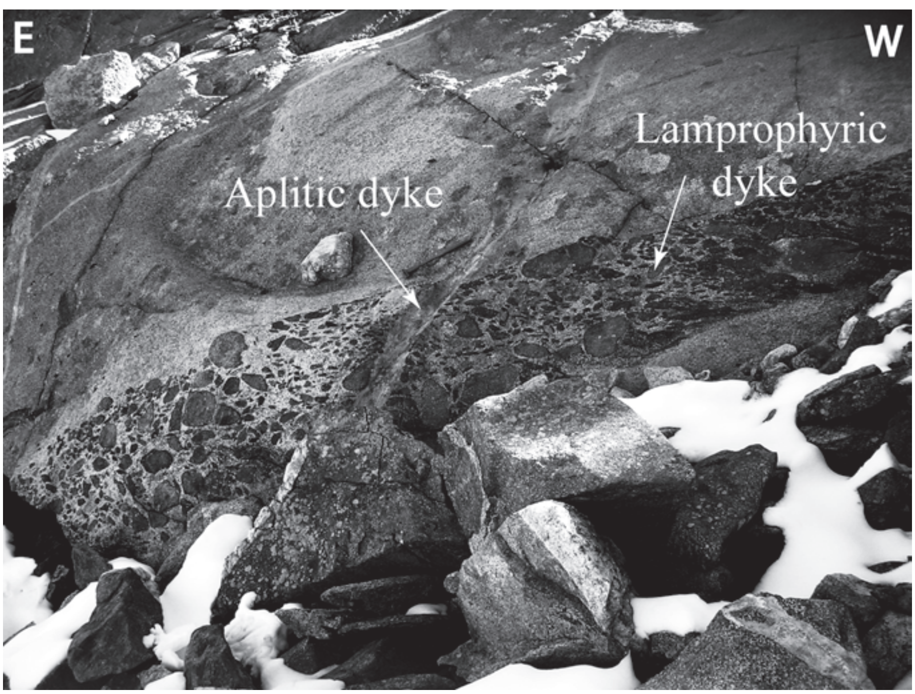

Fig. 7. Swarm of mafic enclaves of lamprophyric composition in Matorello gneiss, crosscut sub-vertically by an aplitic dyke (Pne dei Laghetti area, 688'310/147'095).

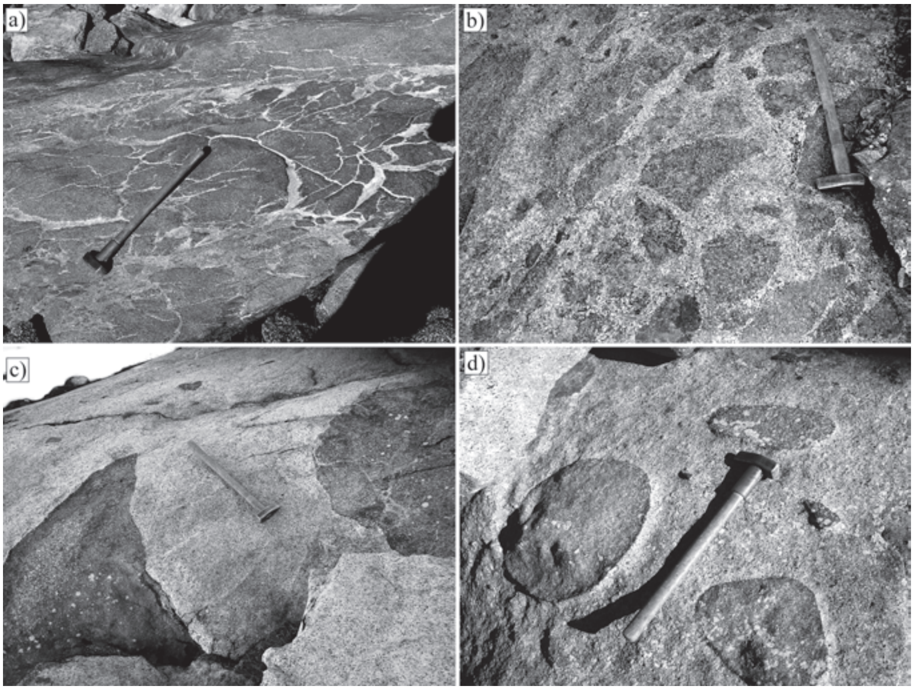

Fig. 8. Different stages of stoping observed in the Pne dei Laghetti area: a) quartz-diorite with thin granitic injection dykes (Swiss co-ordinates 688'460/147'243). b) Angular blocks of quartz-diorite surrounded by granitic dykes but still fitting together (688'380/147'158). c) Completely separated, more rounded blocks of quartz-diorite, 5 cm to 1.5 m in size, in Matorello gneiss (688'357/147'137). d) Isolated, sub-ellipsoidal blocks of quartz-diorite in Matorello gneiss (688'362/147'115).

gneiss, where the deformation is heterogeneous and the influence of D_2 is weaker, is S_1 locally preserved as the dominant schistosity (e.g. Simpson 1982a). In this lithology, which was not pervasively layered or foliated prior to Alpine deformation, D_1 is characterized by spectacular heterogeneous ductile shear zones (Ramsay & Graham 1970; Simpson 1982a; Ramsay & Allison 1979). In other, layered rock types, D_1 is represented by isoclinal folds with thickened hinges, overprinted by the younger deformation phases (Fig. 9a). The occurrence of D_1 folds within the Mesozoic calc-micaschists establishes an Alpine age for this deformational event.

5.2. Deformation phase D_2

Except for the region of the Matorello gneiss, D_2 is the strongest deformation phase throughout the Naret region and produced a pervasive refolding of the D_1 nappe stack on a regional scale. D_2 developed tight to isoclinal folds in both layering (S_0) and S_1 (Figs. 9a, 9b), with the formation of a penetrative fold axial plane foliation S_2. Because of the isoclinal F_2 geometry, layering, S_1 and S_2 are effectively parallel on the limbs of F_2 folds, and limb zones generally predominate on both the outcrop and regional scale. The main regional foliation is, therefore, a composite ($S_0 + S_1 + S_2$) parallel to S_2 (Grujic & Mancktelow 1996; Maxelon & Mancktelow 2005). However, in the hinge regions of D_2 folds it can be shown that the folded layering and S_1 are commonly more strongly developed than the new axial plane foliation S_2 (e.g. Rütti et al. 2005).

In the study area, S_2 generally dips steeply to the NNW (Figs. 3, 10, 12), reflecting the location of the Naret region in the Northern Steep Zone of Milnes (1974b). Only at Passo del Sasso Nero and near P. di Mezzodì does S_2, influenced by D_3 (section 6.2), show an abrupt change in this trend (Figs. 3, 10).

D_2 produces a strong mineral/stretching lineation (L_2), defined by elongated quartz, feldspar and, especially, biotite crystals. Generally, L_2 is subparallel to the F_2 fold axes and plunges to NNE-ENE (Figs. 3, 12). L_2 is related to a widely developed top-to-NE shearing, which produces a locally penetrative S-C' fabric and asymmetric σ-clasts (Figs. 9c, 9d). When not overprinted by later D_3 or D_4 folding, F_2 axes are generally straight on the outcrop scale and there is no field evidence for F_2 sheath-fold development in the Naret area. If F_2 axes were rotated toward the stretching direction as the result of progressive shear (e.g. Sanderson 1973), then they were all rotated in the same sense, without the development of curved hinges and sheath-like geometries.

5.3. Deformation phase D_3

D_3 developed open and more upright folds, with axes approximately coaxial with F_2. The folds are often disharmonic in style and have an overall corrugated form, with a much lower amplitude to wavelength ratio when compared to F_1 and F_2 (cf. Grujic & Mancktelow 1996). The trend of D_3 folds is oblique to the main trend of the Alps and these folds were referred to as "crossfolds" or "Querfalten" in the older literature (e.g. Preiswerk 1921). A crenulation cleavage S_3 is locally developed in the hinges of D_3 folds, outlined by new biotite growth (Fig. 9e). A more pervasive S_3 foliation is only observed at Passo del Sasso Nero, in the hinge zone of the large D_3 Peccia synform (Fig. 16). As a result of the subsequent D_4

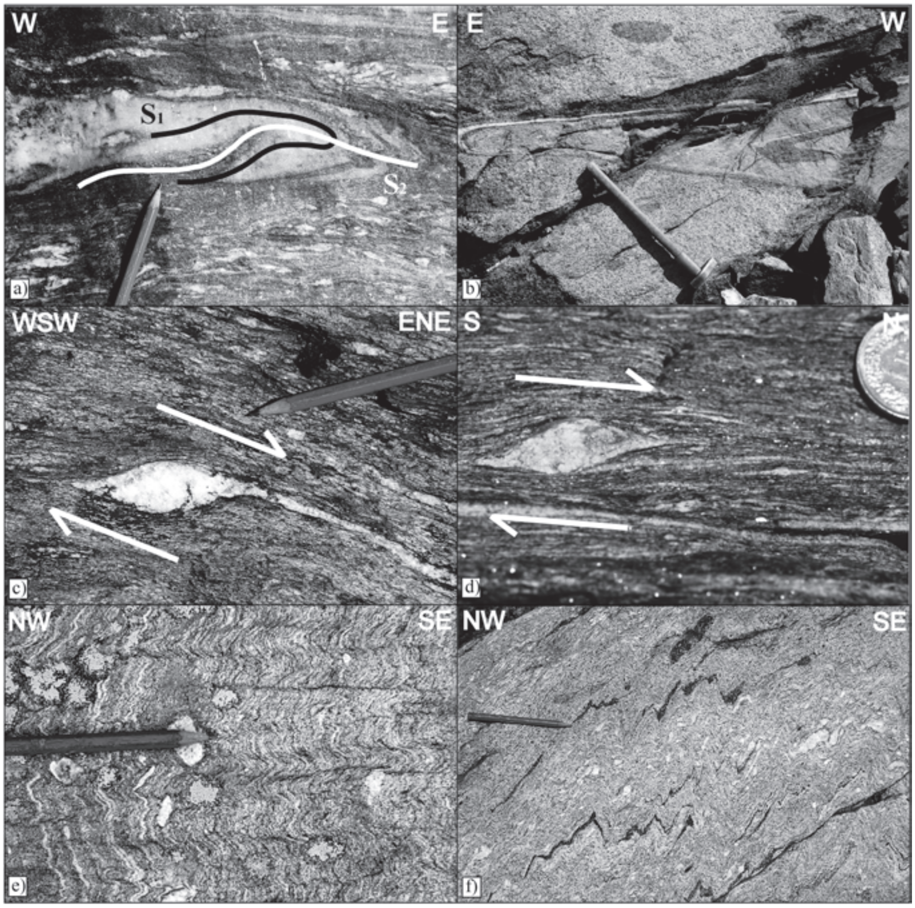

Fig. 9. Deformation patterns produced during D_1, D_2, D_3 and D_4. a) D_1 isoclinal fold, overprinted isoclinally and coaxially by a D_2 fold, in a calc-micaschist of the Bedretto Zone (near Garzonera, 689'604/140'770). b) D_1 shear zone in the Matorello gneiss folded around a tight D_2 fold (Pne dei Laghetti area, 688'582/147'267). c) Quartz σ-clast within the main foliation S_2, showing a top-to-NE sense of shear (Lebendun nappe, near Lago del Fornà, 687'183/149'029). d) Feldspar σ-clast showing a top-to-NE sense of shear (Maggia nappe, near Lago del Naret, 687'277/147'870). e) Parasitic, cm-scale open D_3 folds in the hinge zone of the D_3 Peccia synform, developing a new D_3 crenulation cleavage perpendicular to the main foliation S_2 (orthogneiss of the Maggia nappe, near Passo del Sasso Nero, 686'135/147'041). f) Open and disharmonic D_4 parasitic folds in the Matorello gneiss (Pne dei Laghetti area, 688'555/147'177) with sharp hinges and chevron shapes.

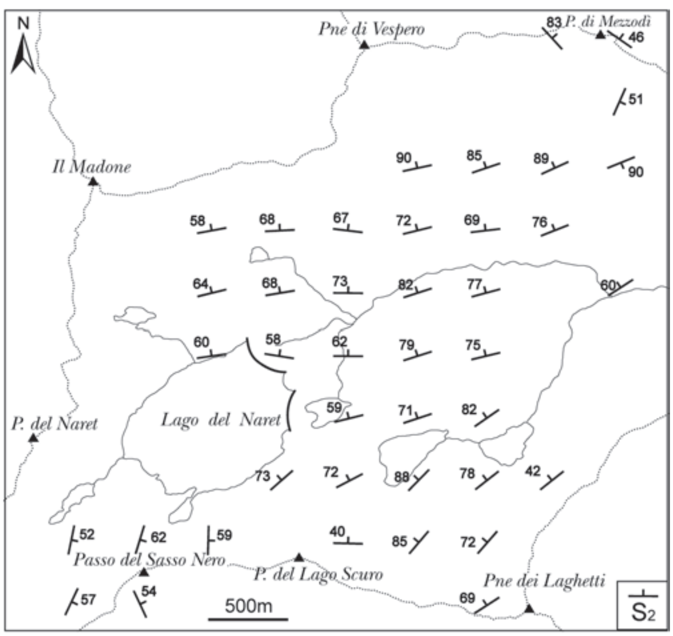

Fig. 10. Structural map of S_2 foliations in the study area. 1254 field measurements of S_2 were averaged with inverse distance weighted spatial averaging, using the program SpheriStat 2.1c (Pangaea Scientific, 1997).

overprint, S_3 dips to the NNE in the SW of the study area and to the NE in the NE of the area (Figs. 3, 11a). D_3 produced a well developed crenulation lineation throughout the study region, whose orientation changes progressively from NNE in the SW to ENE in the NE (Figs. 3, 11b).

5.4. Deformation phase D_4

D_4 is an open folding phase responsible for the development of the Northern Steep Zone (Fig. 1; Milnes 1974b). The folding style is very similar to D_3. D_4 folds are open and disharmonic, with sharp or rounded hinges (Fig. 9f). However, the two deformation phases are easily distinguishable because of their different orientation. In fact, F_4 axial planes develop more or less perpendicular to the F_3 axial planes in the whole area, having a relatively constant orientation dipping to NW (Figs. 2b, 12). F_4 axes plunge to NE (Figs. 2b, 12). In rare cases, a weakly developed crenulation cleavage is observed in the hinges of D_4 folds, marked by the syn-tectonic growth of biotite and muscovite. There is no direct evidence for a superimposition of D_4 on D_3 in the Naret area but, from the structural maps of Fig. 11, it can be seen that D_4 folds S_3 and L_3 on the map scale.

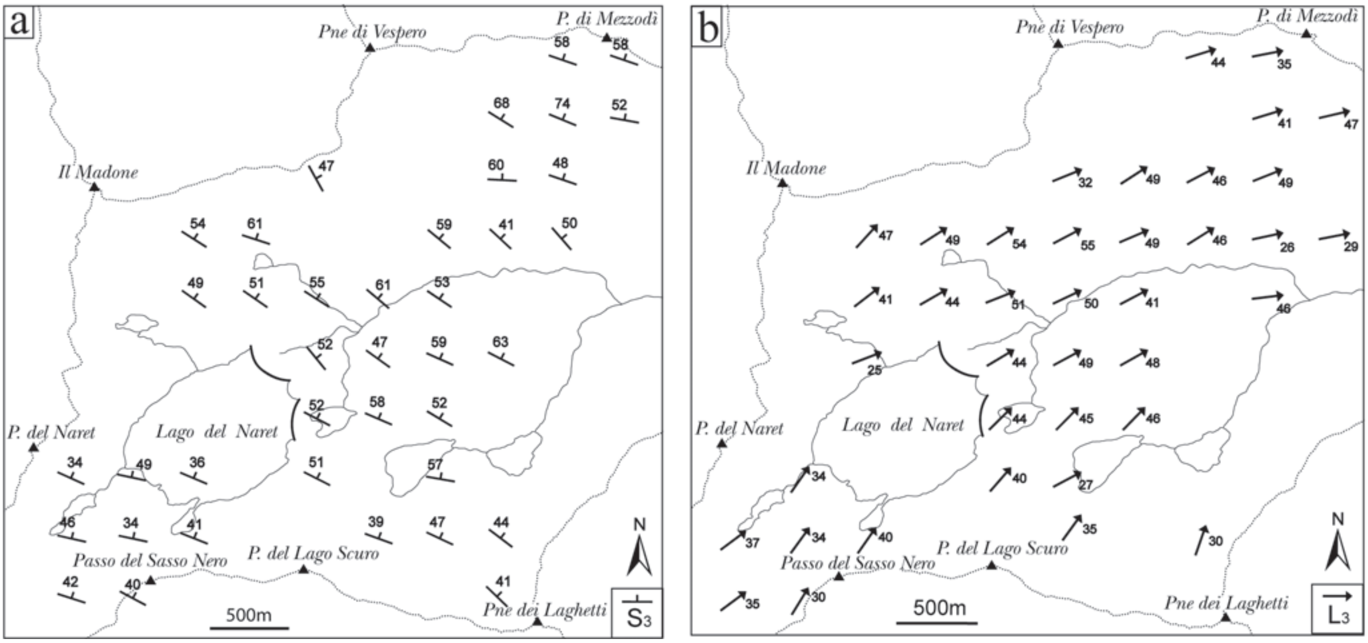

Fig. 11. Structural maps of S_3 foliations (a) and L_3 crenulation lineation (b). 341 field measurements of S_3 and 775 field measurements of L_3 were averaged with inverse distance weighted spatial averaging, using the program SpheriStat 2.1c (Pangaea Scientific, 1997).

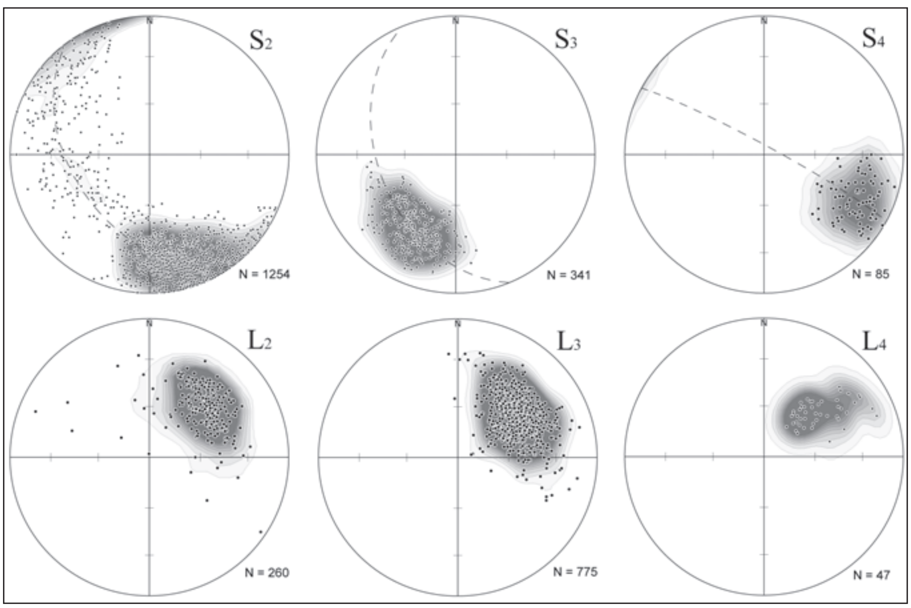

Fig. 12. Stereographic projections (lower hemisphere) of planar and linear elements of D_2, D_3 and D_4. N: number of structural data points. S_2, S_3, S_4 poles of the foliation.

5.5. Interference patterns

Although, the characteristics of individual fold phases have been discussed separately, the geometry from outcrop to map scale is finally determined by the characteristic interference patterns that developed as a result of fold superposition. The fold interference pattern classification used here to discuss the final geometry follows that of Ramsay (1967) and Ramsay & Huber (1987).

In the field, it is only possible to observe superposition between D_1, D_2 and D_3. As noted above, the overprinting caused by D_4 is not seen directly on the outcrop scale but can be interpreted from stereographic projections (Fig. 12) and from the map pattern of S_3 and L_3 (Figs. 11a, 11b).

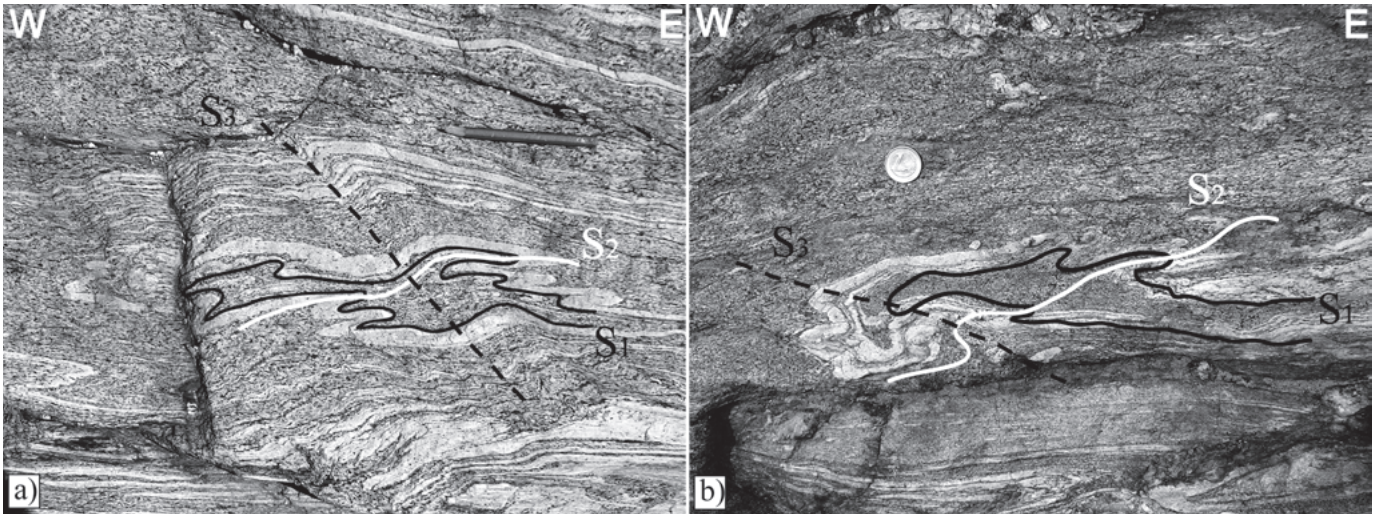

Fig. 13. Examples of interference structures between D_1, D_2 and D_3, in paragneisses of the Maggia nappe. a) Interference pattern of Type 2 (mushroom) between D_1 and D_2 (near Lago del Naret, 687'322/147'568). b) Coaxial interference pattern of Type 3 between D_1 and D_2 (near Lago Scuro, 687'444/147'883).

Fig. 13 illustrates both types of fold interference pattern observed in the studied area. In Fig. 13a, F_1 and S_1 are overprinted by isoclinal D_2 folding, with the F_2 axis oblique to that of F_1 (i.e. the folding is not coaxial), resulting in a tightening of F_1 and the local development of a Type 2 (mushroom) interference pattern. In contrast, the subsequent open overprint by D_3 forms F_3 folds that are coaxial with F_2, to produce an interference pattern of Type 3.

In Fig. 13b, the superposition history is somewhat different. S_1 is again isoclinally folded by D_2 but, in this case, F_1 and F_2 are effectively coaxial. As a result, there is no closure of layering and S_1 in opposite directions to form a mushroom shape. Instead, an interference pattern of Type 3 is developed. Subsequent open folding by D_3, directly comparable to the previous example, is coaxial and again produces an interference pattern of Type 3.

In summary, the superposition of D_2 on D_1 can produce interference patterns of both Type 2 and Type 3, implying that folding was not always coaxial. However, F_3 is always coaxial with F_2 and only producing Type 3 interference patterns.

6. Tectono-stratigraphic reconstruction

As noted in the introduction, a tectono-stratigraphic reconstruction of the northern Lepontine area is not straightforward and remains controversial. The major problem, which was also encountered in the current study, is in scaling-up the outcrop-scale observations on fold interference geometry and fold vergence to the dimensions of individual nappe units. This is made particularly difficult by the fact that F_1 and F_2 fold overprinting was generally not coaxial. The large-scale geometry is therefore truly 3D and the lack of a unique and consistent line of projection implies that the true geometry is not readily transformed into the usual 2D profiles (cf. Maxelon & Mancktelow 2005). In spite of these limitations, this section attempts to develop a regional model of the nappe evolution in the Naret region, with emphasis on the geometry and position of the Lebendun nappe.

6.1. Lebendun nappe

6.1.1. Field observations

As shown in Fig. 14, the geometry of the Lebendun nappe is complex. North of the Lago del Fornà, as well as south and east of Garzonera, the northern boundary between the Lebendun nappe and the Mesozoic rocks is folded isoclinally with a consistent S vergence (note that all vergences are reported looking down, along the fold axis). Southeast of Campanile, the same boundary is also strongly folded but the fold vergence is now Z. In contrast, the southern Lebendun boundary is generally straight and without parasitic folds. Only east of Garzonera is it folded isoclinally with an S vergence. Moreover, south of P. di Mezzodì, all the lithologies are overprinted by an open folding phase, with a fold axial plane dipping moderately NE.

In the adjacent calc-micaschists, D_2 folds south of the Lebendun nappe and near Garzonera are clearly Z-vergent, while east of Lago del Fornà they have an S vergence.

6.1.2. Tectonic interpretation

The symmetric Mesozoic-Lebendun-Mesozoic structure implies that the rocks of the Lebendun nappe lie in the core of a major isoclinal fold. In agreement with Maxelon (2004), we interpret this structure as a D_1 anticline, the Lebendun-nappe anticline, formed during nappe stacking, as the Maggia nappe was thrust over the Lebendun nappe (Fig. 15a). The Z-vergent isoclinal folds southeast of Campanile and the S-vergent fold

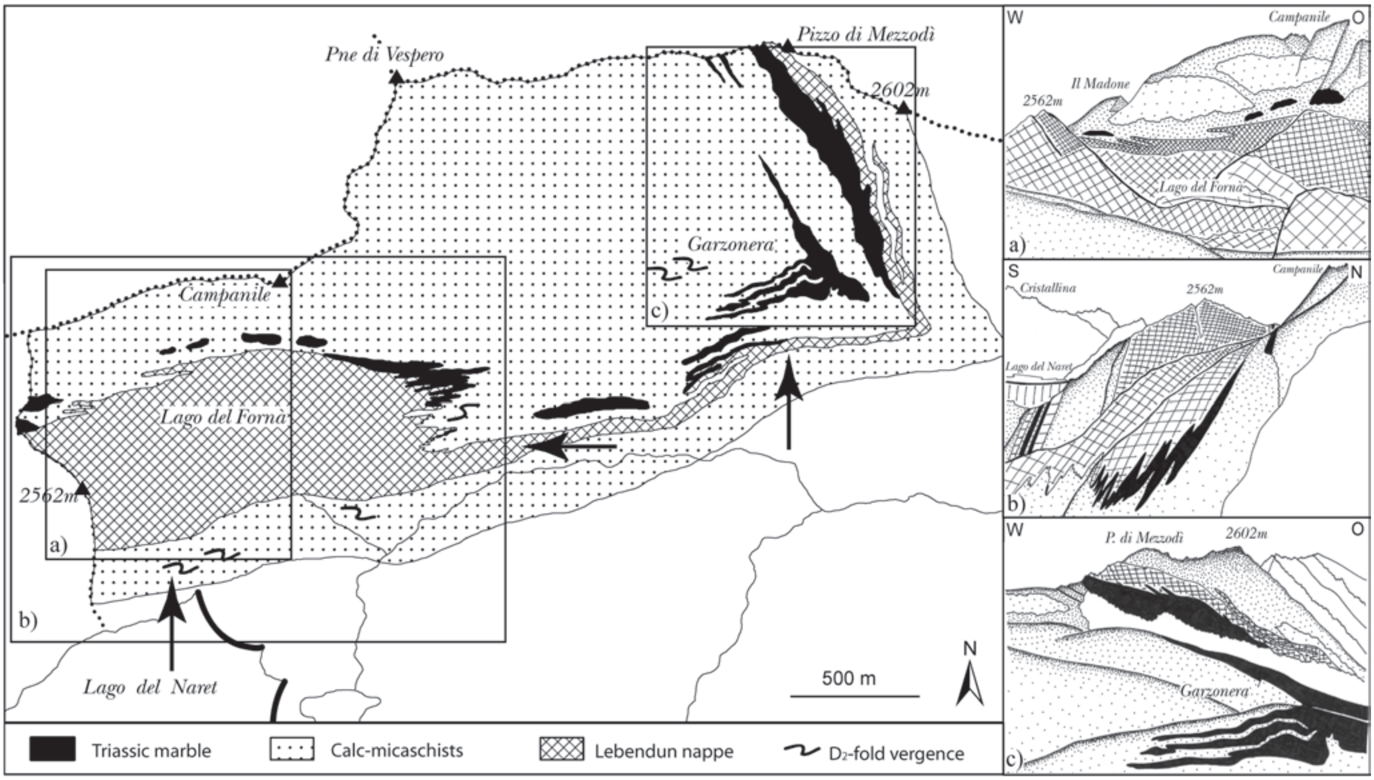

Fig. 14. Tectonic map showing the Lebendun nappe boundary geometry and the main vergences of the D_2 folds. a) Sketch of the geological situation at Lago del Fornà. b) Sketch of the geological situation SE of Campanile. c) Sketch of the geological situation at Garzonera. Arrows indicate the viewing directions. Lithological signatures are the same as in Fig. 2a.

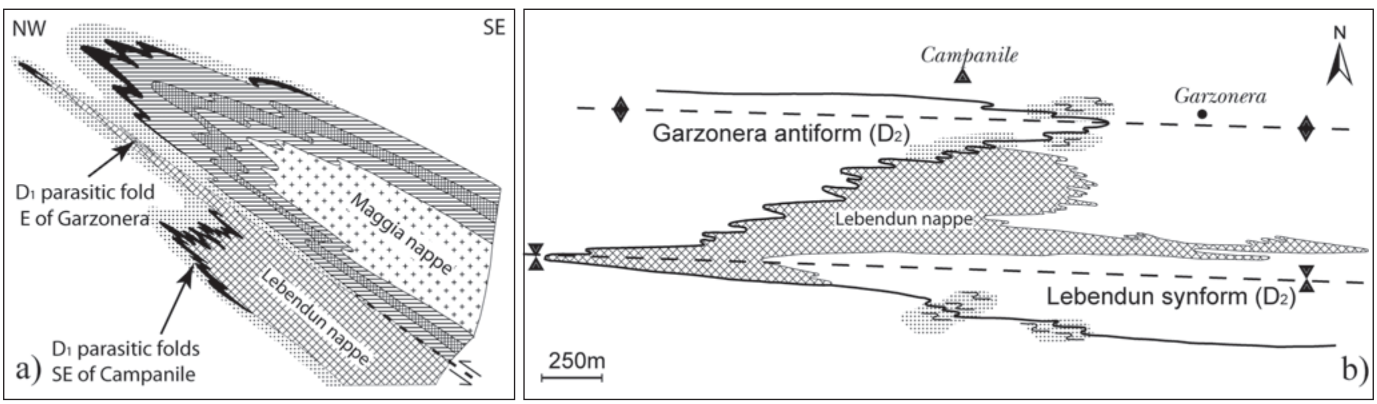

Fig. 15. a) Tectonic situation after D_1 thrusting of the Maggia nappe over the Lebendun nappe, showing the main mapped D_1 parasitic folds. b) Tectonic situation after D_2 refolding of the nappe stack, showing the complex Lebendun nappe geometry, the main D_2-fold structures, as well as the vergences of the mapped D_2 parasitic folds. Lithological signatures are the same as in Fig. 2a.

east of Garzonera (Fig. 14) are interpreted as parasitic folds on this D_1 structure.

The S vergences of the isoclinal folds north of the Lago del Fornà as well as south and east of Garzonera (Fig. 14) are not consistent with a D_1 antiform. These folds are therefore interpreted as D_2 folds, superimposed on the pre-existing nappe stack.

Mapping of D_2-fold vergences in the Naret area outlines a series of D_2 structures (Fig. 15b): the Garzonera antiform and the Lebendun synform, which are parasitic structures of the major Bedretto synform to the north, and the Maggia antiform to the south (Maxelon 2004). Since the rocks of the Lebendun nappe do not occur on the southern limb of the Lebendun synform, we conclude that the Lebendun-nappe geometry is the result of a non-coaxial Type 2 (mushroom) interference structure between D_1 and D_2 (Fig. 15b), exactly as is observed on the outcrop scale (Fig. 13a). Open and coaxial D_3 folding is then responsible for folding of all the lithologies south of P. di Mezzodì. The last D_4 phase in turn produces an open fold in the D_3 axial planes and is also responsible for the overall steep orientation in this area (the Northern Steep Zone, Milnes 1974b).

6.2. Summary of the regional tectono-structural evolution

The first deformation phase D_1 led to the formation of large nappes with cores of crystalline basement surrounded by sediments of Mesozoic age (Ayrton & Ramsay 1974). In the study area, D_1 caused thrusting of rocks of the Maggia nappe over those of the Lebendun nappe. The Mesozoic rocks of the Bedretto zone occur in a synclinal position, between the Maggia and Lebendun nappes (Fig. 15a). In agreement with Maxelon (2004), we consider the main D_1 structure to be the Lebendun-nappe anticline, whose parasitic folds are the isoclinal folds SE of Campanile. From the map of Fig. 14, we see that the rocks of the Lebendun nappe are almost exclusively in contact with the Mesozoic calc-micaschists, and Triassic marbles only occur in the D_1 fold hinges. This is probably a result of thickening of marble units in fold hinges during D_1 folding. Since the Lebendun rocks are consistently surrounded by rocks of most likely Triassic and Jurassic age, we interpret them to be of pre-Triassic age (in accordance with Günthert 1954b; Wenk & Günthert 1960; Milnes 1964, 1965; Joos 1969; Bearth 1973; Leu 1986).

The second deformation phase D_2 isoclinally refolded the nappe pile and produced the regional main foliation. In the work area, the major regional-scale D_2 structures recognised are the Bedretto synform and the Maggia antiform (Maxelon 2004), as well as their parasitic folds, the Garzonera antiform and the Lebendun synform.

D_3 is characterised by an open folding phase, responsible for rotation of the main foliation around P. di Mezzodì and Passo del Sasso Nero. This change in orientation is an expression of the Mezzodì antiform and of the Peccia synform, which are parasitic structures on the regional Ticino culmination to the east and on the Maggia Steep Zone to the west (cf. Merle et al. 1989; Maxelon & Mancktelow 2005).

D_4 manifests itself as an open folding phase. It causes the rotation of both S_3 and L_3 and leads to the formation of the Northern Steep Zone (Milnes 1974b). Similar late fold structures have been described further east in the region of the Lukmanier pass, where they have been related to the major Chiera synform that produces the Northern Steep Zone on its northern limb (Milnes 1976; Milnes & Pfiffner 1980; Etter, 1986; Grujic & Mancktelow 1996; Maxelon 2004).

A synthesis of the relationship between the main structures of D_2, D_3 and D_4 is presented in Fig. 16.

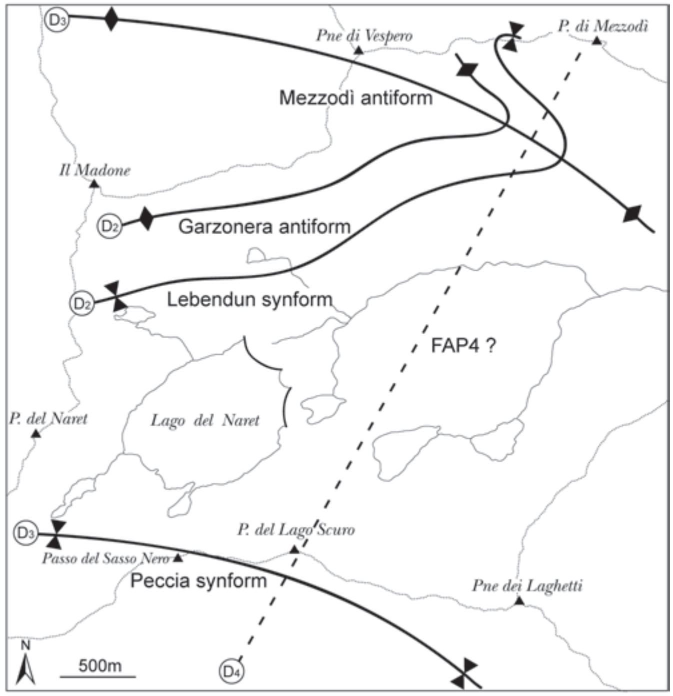

Fig. 16. Structural map of axial plane traces for the major D_2, D_3 and D_4 structures in the Naret region. The exact position of the axial plane trace FAP_4 is uncertain.

7. Metamorphism

Widespread porphyroblastic mineral growth occurred in pelitic rocks of the Maggia nappe and in calc-micaschists of the Bedretto zone, whereas the metapsammitic rocks of the Lebendun nappe are generally porphyroblast-free. Interpretation in thin-section of the relationship between metamorphic mineral growth and microstructures, and the phases of deformation established on a regional scale, allows the relative timing of the Alpine metamorphic history to be established.

7.1. Mineral growth vs. deformation

In the metasedimentary rocks of the Maggia nappe, garnet occurs in two distinct generations (Fig. 17a). Grt_1 is defined by coarse-grained (6–7 mm) idioblastic crystals which predate the main regional deformation phase D_2. Grt_2 is fine-grained (≤ 1.5 mm) and grew between D_2 and D_3 (Fig. 17b). Staurolite porphyroblasts are up to 2 mm in size, grew between D_2 and D_3 and are in apparent equilibrium with grt_2, tourmaline and biotite. A second, less common, staurolite generation postdates D_3, overgrowing the S_3 crenulation cleavage. Plagioclase occurs as poikilitic, coarse-grained (up to 7 mm) porphyroblasts, developing syn- to post-D_3.

The calc-micaschists of the Bedretto zone, contain just a single generation of garnet. Porphyroblasts are idiomorphic, fine to very coarse-grained (0.25 mm–1.5 cm), and chemically

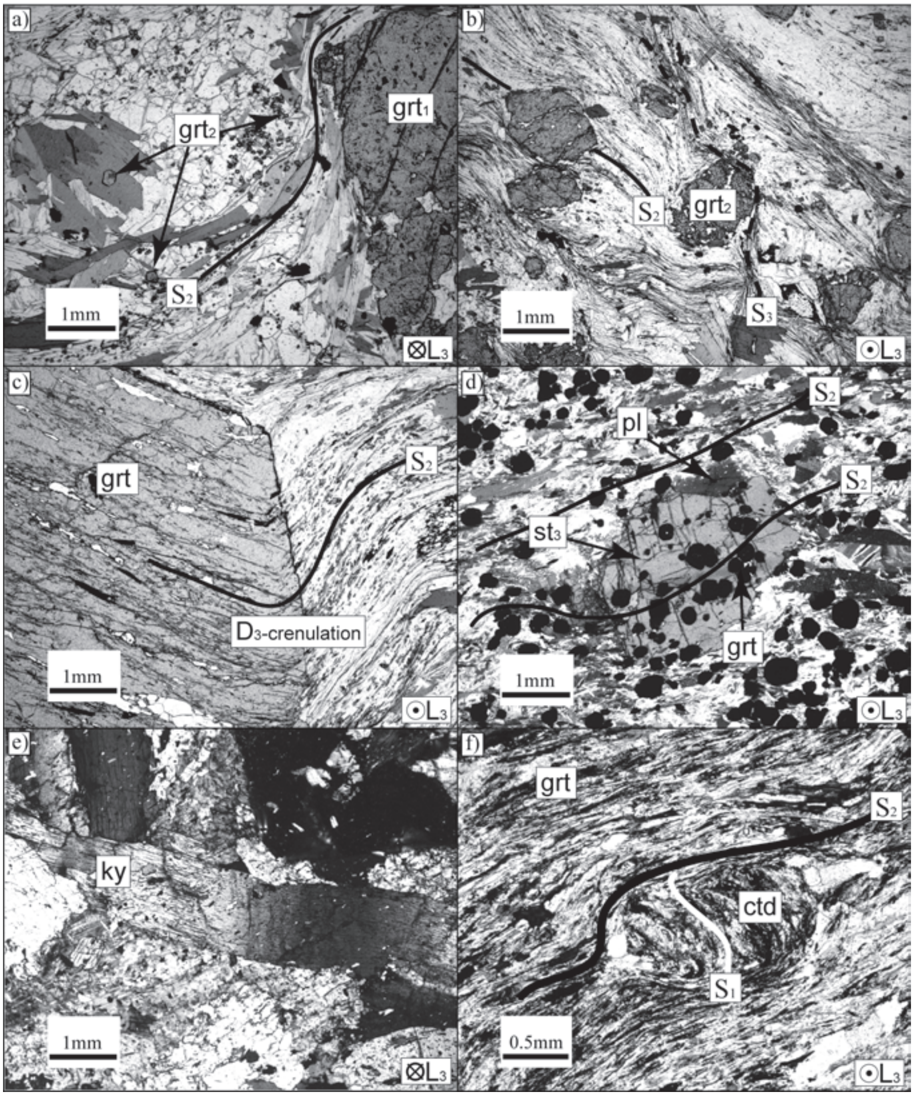

Fig. 17. Photomicrographs showing the relationship between porphyroblast growth and polyphase deformation in metasedimentary rocks of the Maggia nappe and calc-micaschists of the Bedretto zone. a) Two garnet generations in micaschist of the Maggia nappe. The main foliation S_2 is bent around the coarse grained, pre-D_2 grt_1. In contrast, the very fine grained grt_2 overgrows S_2 and therefore postdates D_2. b) S_3 crenulation cleavage deflection around grt_2, showing that grt_2 has grown between D_2 and D_3 (Maggia nappe). c) D_3 folds included in the outernmost rim area of garnet porphyroblast, showing a rim growth post-D_3. The straight inclusion pattern in the inner rim area and in the core indicates a post-D_2 grt-growth (Bedretto zone). d) st_3 growing syn-D_3 and including post-D_2 garnets. Plagioclase overgrew st_3 and postdates therefore D_3. f) Pre-D_2 chloritoid inclusion in garnet (Bedretto zone). Chloritoid includes a relictic S_1 foliation. Therefore, chloritoid has grown between D_1 and D_2. e) Undulos extinguishing pre-D_3 kyanite porphyroblast (Bedretto zone) a,b,c,f: by plane polarised light; d,f: crossed polarised light.

zoned. Mn^{2+} and Ca^{2+} rich crystal cores developed before D_2 and were overgrown by Fe^{2+} and Mg^{2+} rich mantles between D_2 and D_3. Only the outermost rim developed after D_3, overgrowing D_3 crenulation folds (Fig. 17c). Staurolite and kyanite occur exclusively in metapelitic bands within the Bedretto zone calc-micaschists. Fine-grained (≤ 1 mm) staurolite (st_1) is present as pre-D_2 inclusions in garnet. St_2 then grew between D_2 and D_3, in equilibrium with garnet and kyanite (Fig. 6b). St_3 is characterised by coarse-grained porphyroblasts (≤ 4–5 mm), developing syn- to post-D_3 and overgrowing garnet (Fig. 17d). Kyanite porphyroblasts postdate D_2, overgrowing the main foliation S_2 (Fig. 6b). Undulose extinction due to D_3 folding (Fig. 17e), indicates that kyanite porphyroblasts predate D_3. Chloritoid occurs exclusively as fine-grained (≤ 2 mm), pre-D_2 inclusions in garnet. These inclusions contain a relict S_1 foliation which is clearly distinguishable from the main S_2 foliation that deflects around the inclusions (Fig. 17f) and brackets chloritoid growth between D_1 and D_2 phases. Plagioclase porphyroblasts are very coarse in size (up to 8 mm) and, as in the metasedimentary rocks of the Maggia nappe, grew syn- to post-D_3, overgrowing garnet and staurolite (Fig. 17d).

From these observations we conclude that the main stage of mineral growth occurred between D_2 and D_3, both in the metasedimentary rocks of the Maggia nappe and in the calc-micaschists of the Bedretto zone (Table 1). Porphyroblast growth occurred after nappe stacking (D_1) and its subsequent refolding (D_2). These observations are in agreement with the discordant regional trend of metamorphic mineral zones in the Central Alps, which clearly crosscut both D_1 nappe and D_2 regional refold structures (e.g. Niggli & Niggli 1965; Wenk 1970)

7.2. Pressure-temperature evolution

PT histories were established by calculating pseudosections for bulk compositions representing a tourmaline-staurolite-garnet-

Table 1. Relationship between mineral growth and deformation phases in the metasedimentary rocks of the Maggia nappe and in the calc-micaschists of the Bedretto zone.

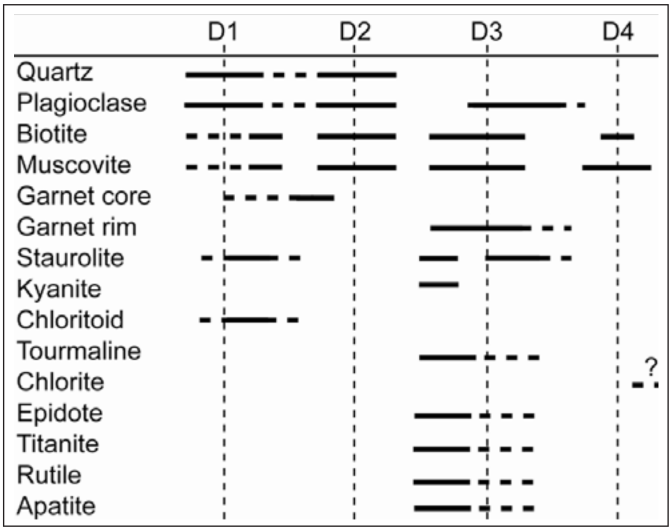

micaschist of the Maggia nappe (Fig. 18a) and a kyanite-staurolite-garnet-micaschist of the Bedretto zone (Fig. 18b). Diagrams were calculated with the 2002 revision of the Holland and Powell thermodynamic dataset (Holland & Powell 1998), the 2005 version of Perplex (Connolly 2005) and appropriate solution-phase models (see Mahar et al. 1997, White et al. 2000, Coggon & Holland 2002, and the Thermocalc(www.esc.cam.ac.uk/astaff/holland/thermocalc.html) and Perplex (www.perplex.ethz.ch/). The Maggia and Bedretto samples were modelled in NaCaMnTiKFMASH and NaCaTiKFMASH systems, respectively, with H_2O in excess in both cases. Melt reactions and ferric iron end-members were not considered (so epidote stability is probably under-represented due to the absence of Fe^{3+}-bearing end-members). Comparison of predicted phase assemblages and observed mineral relations constrains part of the PT evolution of these samples, which are assumed to have a shared Alpine metamorphic history.

A key constraint on the maximum temperatures achieved is that staurolite growth occurred between D_2 and D_3 in both the Bedretto and the Maggia samples, and that although kyanite also grew during the same period, it was restricted to the Bedretto sample. This restricts maximum temperature to between ca. 640°C and 650°C at ca. 8–10 kbar (label 'B' on Figs. 18a, 18b). Fig. 18 demonstrates that both samples may have experienced almost identical Alpine PT histories, with differences in preserved mineral assemblages resulting solely from their different bulk compositions (e.g. Tab. 2).

The occurrence of post-D_1 chloritoid in the Bedretto sample shows only that the temperature during D_1 was lower than

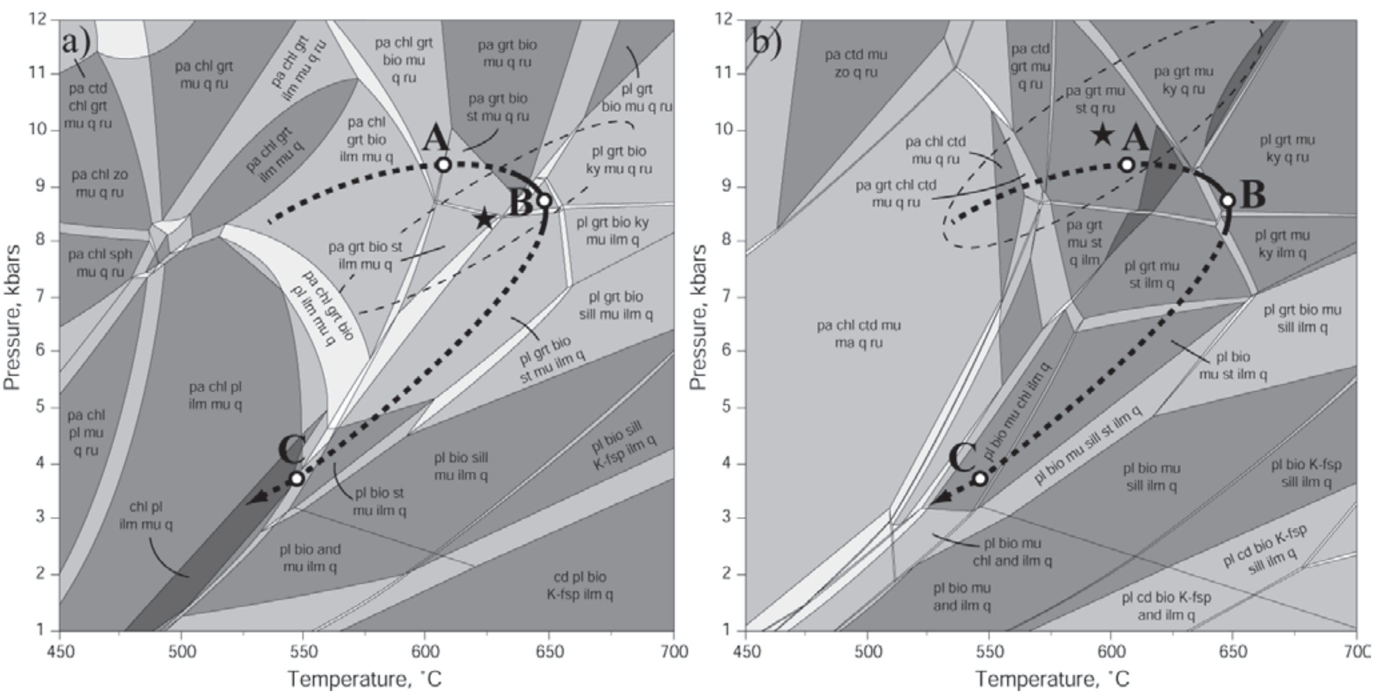

Fig. 18. a) Pseudosection calculated for a bulk composition representing the tourmaline-staurolite-garnet-micaschist of the Maggia nappe (Table 2a) in the system NaCaMnTiKFMASH. b) Pseudosection calculated for a bulk composition representing the kyanite-staurolite-garnet-micaschist of the Bedretto zone (Table 2b) in the system NaCaTiKFMASH. H_2O in excess for both pseudosections. Shading represents assemblage variance (darker = higher variance). Large and petrographically significant fields are labelled. Abbreviations as text except q = quartz, cd = cordierite, ctd = chloritoid, ru = rutile, ilm = ilmenite, sill = sillimanite, and = andalusite, pa = paragonoite, ma = margarite. Stars and dashed ellipses represent THERMOCALC average-PT estimates and their 2σ uncertainties. Bold curves and labelled circles represent constrained PT path and deformation criteria (see text for details).

Table 2. Bulk-rock compositions of a) the tourmaline-staurolite-garnet-micaschist (Maggia nappe) and of b) the kyanite-staurolite-garnet-micaschist (Bedretto zone) used for calculation of the pseudosections (Fig. 18). [c]Total Fe given as FeO; [d]calculated from the loss on ignition.

Rock type	a) Tur-st-grt-micaschist (Maggia nappe)	b) Ky-st-grt-micaschist (Bedretto zone)
Major Elements (wt-%)		
SiO_2	56.54	55.44
TiO_2	0.98	1.46
Al_2O_3	22.79	30.02
Cr_2O_3	0.02	0.02
FeO^c	8.18	5.29
MnO	0.12	0.03
MgO	2.85	0.84
CaO	0.51	1.41
Na_2O	1.28	1.51
K_2O	4.15	3.34
P_2O_5	0.17	0.04
H_2O^d	2.54	1.72
Total	100.13	101.12

the ca. 570 ˚C chloritoid-out reactions (Fig. 18b). Due to the strong overprint of subsequent deformation phases, further reconstruction of the stable mineral assemblage during D_1 and consequent estimation of its PT conditions is difficult.

Syn-kinematic growth of biotite and muscovite but not of chlorite during D_2 implies that D_2 occurred after chlorite-out (e.g. at 610–640°C, 8.5–10 kbar), although D_2 growth and subsequent breakdown of chlorite cannot be discounted.

The occurrence of kyanite instead of sillimanite as the stable aluminosilicate phase in the Bedretto sample allows the lowermost limit of the maximum pressure phase to be constrained at ca. 7 kbar. An estimation of the upper limit of P_{max} cannot be so easily constrained. We suggest that P_{max} was lower than 10 kbar (e.g. at label 'A' in Fig. 18) since there is textural evidence of protracted staurolite growth through D_2, and Fig. 18a implies that higher prograde pressures would result in staurolite growth only as the thermal peak is reached.

PT conditions during D_3 are constrained by the absence of sillimanite and the growth of S_3 staurolite after kyanite and garnet. We propose that D_3 is bracketed by the thermal maximum (which occurred between D_2 and D_3) and the growth of retrograde biotite in the axial plane of D_4 folds during the last deformation phase, which occurred before point 'C' on Figs. 18 a and 18b.

8. Conclusions

The results of this study can be summarized as follows.

1. In the Naret region, three main tectonic units occur: the northern and frontal part of the Maggia nappe, the eastern part of the Lebendun nappe and the Bedretto zone.
2. The Maggia nappe is composed of pelitic to psammitic metasedimentary rocks, orthogneiss and rocks of the Matorello group.
3. Sharp boundaries against the country rocks, the occurrence of mafic enclaves indicating both stoping and magma mingling, and the presence of late intrusive lamprophyric, aplitic and pegmatitic dykes, all indicate a primary magmatic intrusive origin for rocks of the Matorello group, rather than a remobilisation of adjacent gneisses.
4. The Lebendun nappe consists of fine- to medium-grained metasedimentary rocks of arkosic composition. No evidence for conglomeratic sediments has been found in the study area. The position of these rocks consistently below the enveloping Mesozoic metasediments indicates that they are of pre-Triassic age. The complex nappe geometry is the result of non-coaxial interference between D_1 and D_2 folds.
5. The Bedretto zone represents the Mesozoic cover unit of the Maggia and Lebendun nappes. It consists of Triassic calcite and dolomite marbles, as well as heterogeneous calc-micaschists (Bündnerschiefer), which both act as a nappe separator.
6. During Alpine orogenesis, all rocks in the Naret region have been affected by amphibolite-facies metamorphism and by four ductile deformation phases. During D_1 the Maggia nappe was thrust over the Lebendun nappe, with the two units now separated by the Mesozoic metasediments of the Bedretto zone. D_1 produced isoclinal folds and ductile shear zones at estimated temperatures of 500–530°C and pressures of 9–10 kbar. D_2 caused isoclinal refolding of the nappe pile, accompanied by shearing with top-to-NE sense. It also produced the main regional foliation and a stretching lineation parallel to the D_2 fold axis. Estimated conditions of this phase are ca. 610–640°C and 8.5–10 kbar. A thermal peak was attained between D_2 and D_3 and is characterized by garnet, staurolite, kyanite, tourmaline and plagioclase blastesis at ca. 640–650°C, ca. 8–9 kbar. D_3 produced an open crossfolding of the nappe stack and locally developed a penetrative crenulation cleavage in the hinges of D_3 folds and a strong crenulation lineation. The major D_3 structures are the Peccia synform and the Mezzodì antiform. D_4 is an open backfolding phase, responsible for the rotation of S_3 and L_3 and for the development of the Northern Steep Zone. This phase is estimated to have occurred at ≥ 550°C and ≥ 3 kbar.

Acknowledgements

Our heartfelt thanks go to Barbara Kuhn, Michael Maxelon and Roger Rütti for the helpful discussions and to OFIMA for the accommodation during two field summers. We appreciate the comments and helpful reviews of Kurt Krenn and Michael Stipp. We express our sincere thanks to Reto Gieré for his helpful suggestions and the editorial handling of this manuscript.

REFERENCES

Albisetti, D. 1999: Petrografia e geologia strutturale delle falde Maggia e Campo Tencia/Simano nella regione del Campolungo. Unpublished Diploma Thesis, ETH, Zürich.

Allaz, J. & Mader, X. 2003: Evolution tectonique et métamorphique de la nappe de Simano à l'Alpe Larecc, Val Maggia (Tessin, Suisse). Unpublished Diploma Thesis, Uni Lausanne.

Ayrton, S.N. & Ramsay, J. 1974: Tectonic and metamorphic events in the Alps. Schweizerische Mineralogische und Petrographische Mitteilungen 54, 609–639.

Bearth, P. 1973: Erläuterungen zu Blatt Simplon. Erläuterungen zur geologischen Karte der Schweiz. Schweizerische Geologische Kommission (Schweizerische Naturforschende Gesellschaft).

Burckhardt, C. 1942: Geologie und Petrographie des Basodino-Gebietes. Schweizerische Mineralogische und Petrographische Mitteilungen 22, 99–186.

Chappell, B.W. & White, A.J.R. 1974: Two contrasting granite types. Pacific Geology 8, 173–174.

Coggon, R. & Holland, T.J.B. 2002: Mixing properties of muscovite-celadonite-ferroceladonite-paragonite micas and revised garnet-phengite thermobarometers. Journal of Metamorphic Geology 20, 683–696.

Connolly, J.A.D. 2005: Computation of phase equilibria by linear programming: A tool for geodynamic modeling and its application to subduction zone decarbonation. Earth and Planetary Science Letters 236, 524–541.

Etter, U. 1986: Stratigraphische und strukturgeologische Untersuchungen im gotthardmassivischen Mesozoikum zwischen dem Lukmanierpass und der Gegend von Ilanz. Ph.D. thesis, Univiversität Bern

Froitzheim, N., Schmid, S.M. & Frey, M. 1996: Mesozoic paleogeography and the timing of eclogite-facies metamorphism in the Alps: a working hypothesis. Eclogae geologicae Helvetiae 89, 81–110.

Grujic, D. 1992: Superposed folding: analogue models and comparison with natural examples from the Maggia nappe (pennine zone, Switzerland). Ph.D. Thesis, ETH, Zürich.

Grujic, D. 1993: The influence of initial fold geometry on Type 1 and Type 2 interference patterns: an experimental approach. Journal of Structural Geology 15, 293–307.

Grujic, D. & Mancktelow, N. 1996: Structure of the northern Maggia and Lebendun Nappes, Central Alps, Switzerland. Eclogae geologicae Helvetiae 89, 461–504.

Günthert, A. 1954a: Beiträge zur Petrographie und Geologie des Maggia-Lappens (NW-Tessin). Ph.D. Thesis, Univ. Basel.

Günthert, A. 1954b: Beiträge zur Petrographie und Geologie des Maggia-Lappens (NW-Tessin). Schweizerische Mineralogische und Petrographische Mitteilungen 34, 1–159.

Günthert, A., Stern, W. & Schwander, H. 1976: Isochemische Granitgneisbildung im Maggia-Lappen (Lepontin der Zentralalpen). Schweizerische Mineralogische und Petrographische Mitteilungen 56, 105–146.

Günthert, A., Stern, W. & Schwander, H. 1996: The polyciclic evolution of the Penninic Maggia nappe, Central Alps: a summary report. Schweizerische Mineralogische und Petrographische Mitteilungen 76, 1–22.

Gunzenreiner, S. 1998: Petrographie und Strukturgeologie zwischen Maggia und Campo Tencia-Decke im Gebiet des Passo Campolungo. Unpublished Diploma Thesis, ETH, Zürich.

Hill, R. 1984: Petrology and petrogenesis of batholithic rocks, San Jacinto Mountains, S-California. Ph.D. Thesis, California Institute of Technology.

Holland, T.J.B. & Powell, R. 1998: An internally consistent thermodynamic data set for phases of petrological interest. Journal of Metamorphic Geology 16, 309–343.

Huber-Aleffi, A. 1982: Strain determinations in the conglomeratic gneiss of the Lebendun Nappe, Ticino, Switzerland. Geologica Romana 21, 235–277.

Huber, M., Ramsay, J. & Simpson, C. 1980: Deformation in the Maggia and Antigorio nappes, Lepontine Alps. Eclogae geologicae Helvetiae 73, 593–606.

Huber, M. 1981: Geologisch-strukturelle Untersuchungen im Oberen Maggiagebiet (Tessin, Schweiz). Ph.D. Thesis, ETH, Zürich.

Joos, M.G. 1969: Zur Geologie und Petrographie der Monte Giove-Gebirgsgruppe im östlichen Simplon-Gebiet (Novara, Italia). Schweizerische Mineralogische und Petrographische Mitteilungen 49, 277–323.

Klaper, E. 1980: Strukturen, Deformation und Metamorphose in der nördlichen Maggia-Zone. Unpublished Diploma Thesis, ETH, Zürich.

Klaper, E. 1982: Deformation und Metamorphose in der nördlichen Maggia-Zone. Schweizerische Mineralogische und Petrographische Mitteilungen 62, 47–76.

Klaper, E. 1985: Deformation history and metamorphic mineral growth along the Pennine frontal thrust (Wallis, Ticino), Switzerland. Ph.D. Thesis, ETH, Zürich.

Köppel, V., Günthert, A. & Grünenfelder, M. 1981a: Zircon and monazite U/Pb age patterns of polymetamorphic units of the southern Central Swiss Alps. Schweizerische Mineralogische und Petrographische Mitteilungen 61, 23–24.

Köppel, V., Günthert, A. & Grünenfelder, M. 1981b: Patterns of U-Pb zircon and monazite ages in polymetamorphic units of the Swiss Central Alps. Schweizerische Mineralogische und Petrographische Mitteilungen 61, 97–119.

Leu, W. 1986: Litostratigraphie und Tektonik der nordpenninischen Sedimente in der Region Bedretto-Baceno-Visp. Eclogae geologicae Helvetiae 79, 769–824.

Mahar, E., Powell, R., Holland, T. J. B. & Howell, N. 1997: The effect of Mn on mineral stability in metapelites. Journal of Metamorphic Geology 15, 223–238.

Maxelon, M. 2004: Developing a three-dimensional structural model of the Lower Lepontine Nappes-Central Alps, Switzerland and Northern Italy. Ph.D. Thesis, ETH, Zürich.

Maxelon, M. & Mancktelow, N. 2005: Three-dimensional geometry and tectonostratigraphy of the Pennine Zone, Central Alps, Switzerland and northern Italy. Earth-Science Reviews 71, 3–4, 171–227.

Merle, O., Cobbold, P.R. & Schmid, S. 1989: Tertiary kinematics in the Lepontine dome. In: Alpine Tectonics (edited by Coward, M. P., Dietrich, D. & Park, R. G.), Geological Society of London Special Publication 45, 113–134.

Milnes, A. 1964: Structure and history of the Antigorio nappe (Simplon group, North Italy). Ph.D. Thesis, Univ. Basel.

Milnes, A. 1965: Structure and history of the Antigorio nappe (Simplon Group, North Italy). Schweizerische Mineralogische und Petrographische Mitteilungen 45, 167–177.

Milnes, A. 1974a: Post-nappe folding in the western Lepontine Alps. Eclogae geologicae Helvetiae 67, 333–348.

Milnes, A. 1974b: Structure of the Pennine Zone (Central Alps): a new working hypothesis. Bulletin of the Geological Society of America 85, 1727–1732.

Milnes, A.G. 1976: Strukturelle Probleme im Bereich der Schweizer Geotraverse – das Lukmanier-Massiv. Schweizerische Mineralogische und Petrographische Mitteilungen 56, 615–618.

Milnes, A.G. & Pfiffner, O.A. 1980: Tectonic evolution of the Central Alps in the cross section St. Gallen-Como. Eclogae geologicae Helveticae 73, 619–633.

Mohanty, S. & Ramsay, J. 1994: Strain partitioning in ductile shear zones: an example from a Lower Pennine nappe of Switzerland. Journal of Structural Geology 16, 663–676.

Niggli, P., Preiswerk, H., Günthert, O., Bossard, L. & Kündig, E. 1936: Geologische Beschreibung der Tessiner Alpen zwischen Maggia- und Bleniotal. Beiträge zur geologischen Karte der Schweiz. A. Franke AG (Stämpfli & Ge), Bern.

Niggli, E. & Niggli, C. 1965: Karten der Verbreitung einiger Mineralien der alpidischen Metamorphose in den Schweizer Alpen (Stilpnomelan, Alkali-Amphibol, Chloritoid, Staurolith, Disthen, Sillimanit). Eclogae geologicae Helvetiae 58, 335–368.

Preiswerk, H. 1918: Geologische Beschreibung der Lepontinischen Alpen, zweiter Teil: oberes Tessin- und Maggiagebiet. A. Franke, Bern.

Preiswerk, H. 1921: Die zwei Deckenkulminationen Tosa-Tessin und die Tessiner Querfalte. Eclogae geologicae Helveticae 16, 485–496.

Ramsay, J. 1967: Folding and fracturing of rocks. McGraw-Hill, New York.

Ramsay, J. & Graham, R. 1970: Strain variation in shear belts. Canadian Journal of Earth Sciences 7, 786–813.

Ramsay, J. & Allison, I. 1979: Structural analysis of shear zones in an alpinised hercynian granite (Maggia-Lappe, Pennine zone, Central Alps). Schweizerische Mineralogische und Petrographische Mitteilungen 59, 251–279.

Ramsay, J. & Huber, M. 1987: The techniques of modern structural geology. Volume 2: folds and fractures. Academic Press.

Rodgers, J. & Bearth, P. 1960: Zum Problem der Lebendundecke. Eclogae geologicae Helveticae 53(1), 169–178.

Rütti, R. 2003: The tectono-metamorphic evolution of the northwestern Simano nappe (Central Alps, Switzerland). Ph.D. Thesis, ETH, Zürich.

Rütti, R., Maxelon M. & Mancktelow, N. S. 2005: Structure and kinematics of the northern Simano Nappe, Central Alps, Switzerland. Eclogae geologicae Helvetiae 98, 63–81.

Sanderson, D.J. 1973: The development of fold-axes oblique to the regional trend. Tectonophysics 16, 55–70.

Schmid, C. & Preiswerk, H. 1908: Erläuterungen zur Geologischen Karte der Simplongruppe. A. Franke, Bern.

Schmid, S.M., Fügenschuh, B., Kissling, E. & Schuster, R. 2004: Tectonic map and overall architecture of the Alpine orogen. Eclogae geologicae Helvetiae 97, 93–117.

Simpson, C. 1981: Ductile shear zones: a mechanism of rock deformation in the orthogneisses of the Maggia nappe, Ticino. Ph.D. Thesis, ETH, Zürich.

Simpson, C. 1982a: Strain and shape-fabric variations associated with ductile shear zones. Journal of Structural Geology 5, 61–72.

Simpson, C. 1982b: The structure of the northern lobe of the Maggia nappe, Ticino, Switzerland. Eclogae geologicae Helveticae 75, 495–516.

Spring, L., Reymond, B., Masson, H. & Steck, A. 1992: La nappe du Lebendun entre Alte Kaserne et le Val Cairasca (massif du Simplon): nouvelles observations et interprétations. Eclogae geologicae Helvetiae 85, 85–104.

Steck, A. & Hunziker, J. 1994: The Tertiary structural and thermal evolution of the Central Alps – compressional and extensional structures in an orogenetic belt. Tectonophysics 238, 229–254.

Steck, A. 1998: The Maggia cross-fold: an enigmatic structure of the lower Penninic nappes of the Lepontine Alps. Eclogae geologicae Helvetiae 91, 333–343.

Steiner, H. 1984a: Radiometrische Alterbestimmungen an Gesteinen der Maggia-Decke (Penninikum der Zentralalpen). Schweizerische Mineralogische und Petrographische Mitteilungen 64, 227–259.

Steiner, H. 1984b: Mineralogisch-petrographische, geochemische und isotopengeologische Untersuchungen an einem Meta-Lamprophyr und seinem granodioritischen Nebengestein (Matorello-Gneis) aus der Maggia-Decke. Schweizerische Mineralogische und Petrographische Mitteilungen 64, 261–271.

Steinmann, M.C. 1994: Die nordpenninischen Bündnerschiefer der Zentralalpen Graubündens: Tektonik, Stratigraphie und Beckenentwicklung. Ph.D Thesis, ETH, Zürich.

Trommsdorff, V. 1966: Progressive Metamorphose kieseliger Karbonatgesteine in den Zentralalpen zwischen Bernina und Simplon. Schweizerische Mineralogische und Petrographische Mitteilungen 46, 431–460.

Wenk, E. & Günthert, A.W. 1960: Über metamorphe Psephite der Lebendun-Serie und der Bündnerschiefer im NW-Tessin und Val Antigorio. Ein Diskussionsbeitrag. Eclogae geologicae Helveticae 53, 179–188.

Wenk, E. 1970: Zur Regionalmetamorphose und Ultrametamorphose im Lepontin. Fortschritte der Mineralogie 47, 34–51.

White, R.W., Powell, R., Holland, T.J.B. & Worley, B. 2000: The effect of TiO_2 and Fe_2O_3 on metapelitic assemblages at greenschist and amphibolite facies conditions: mineral equilibria calculations in the system K_2O-FeO-MgO-Al_2O_3-SiO_2-H_2O-TiO_2-Fe_2O_3. Journal of Metamorphic Geology 18, 497–511.

Manuscript received 29 March 2006
Revision accepted 5 January 2007
Published Online First May 3, 2007
Edtitorial handling: Reto Gieré